ACS Photonics

Article

pubs.acs.org/journal/apchd5

Responsive Colloidal Crystal for Spectrometer Grating

Haibo Ding,[†] Cihui Liu,[†] Hongcheng Gu,[†] Yuanjin Zhao,*[,†,‡] Baoping Wang,[§] and Zhongze Gu*[,†,‡]

[†]State Key Laboratory of Bioelectronics, School of Biological Science and Medical Engineering, and [§]School of Electronic Science and Engineering, Southeast University, Nanjing 210096, China

[‡]Laboratory of Environment and Biosafety, Research Institute of Southeast University in Suzhou, Suzhou 215123, China

Supporting Information

ABSTRACT: Diffraction gratings have a demonstrated value in optical applications, such as monochromators and spectrometers. Recent efforts have been directed at finding simple ways to manufacture diffraction gratings at low cost and under mild conditions. Here we present a practical strategy to fabricate a diffraction grating by simply treating an elastic photonic crystal film with a gradient of stress. The film was made of non-close-packed colloidal crystal arrays embedded in hydrogel polymer. Its photonic band gap (PBG) could be tuned precisely by using varying levels of pressure. Thus, when the elastic photonic crystal film was subjected to a stress gradient, a novel diffraction grating with continuously varying PBGs in the whole visible range could be achieved. The practical application of this type of diffraction grating was demonstrated in a miniaturized spectrometer system.

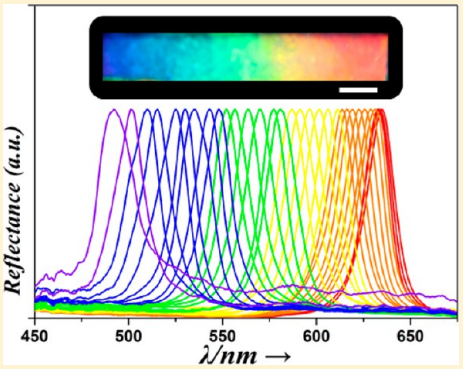

KEYWORDS: *diffraction grating, photonic crystal, colloidal crystal, spectrometer*

INTRODUCTION

Diffraction gratings are optical components with periodic structures. They can diffract light into several beams that travel in different directions depending on the spacing of the grating and the light wavelength.[1−3] Because of this dispersive property, diffraction gratings were found to be valuable in applications such as monochromators and spectrometers. Generally, the spectrometer gratings are fabricated by ruling engines,[4] photolithographic techniques,[5,6] and photosensitive gels.[7,8] With these technologies, different kinds of high-resolution gratings can be manufactured. However, these methods usually have high fabrication costs and harsh processing and are time-consuming. In addition, environmental susceptibility is a trade-off, as some fabrication procedures are conducted at low temperature and high humidity. Therefore, new approaches for generating diffraction gratings are still anticipated.

Colloidal crystals have long been used to construct various three-dimensional (3D) photonic crystal (PhC) materials.[9−13] They can be fabricated simply under a mild environment.[14,15] The periodic variation in refractive index of the colloidal PhC materials creates a forbidden gap in the photonic band structure that reflects light within a specific range of wavelengths and transmits all others.[16−19] Such photonic band gap (PBG) materials are attractive optical materials for controlling and manipulating the transmission of light, including lenses, waveguides, reflective mirrors, color pigments, and numerous other optical components.[20−23] In particular, if these highly ordered colloidal crystals are combined with hydrogel polymers, swelling or shrinking upon stimulation of these polymers would lead to a change in the PBGs of the colloidal crystals.[24−28] Thus, it is conceivable that if a polymer colloidal crystal film was under a gradual variation of stimulus, leading to a corresponding gradient shift in the PBGs of the film, a new diffraction grating with the feature of continuously varying PBGs in the whole visible range could be achieved.

Here, we present the desired diffraction grating and demonstrate its proof of concept application in a spectrometer. The diffraction grating was a hydrogel polymer film incorporated with nonclose-packed colloidal PhC arrays. Because the hydrogel polymer was stress-responsive, the PBGs of the film could be tuned precisely by using varying levels of stress. Thus, when an elastic film was subjected to a gradient of stress in a certain direction, the lattice constant of the film decreased correspondingly in the direction of increasing stress. This change imparted the film with continuously varying PBGs and made it a new type of diffraction grating. By combining the diffraction grating film with a photoelectric conversion module, we demonstrated a miniaturized spectrometer system with the spectrum based on the reflection intensity profile at different spatial positions of the colloidal crystal diffraction grating.

RESULTS AND DISCUSSION

In a typical experiment, non-close-packed polymer colloidal crystal films were conceived and fabricated. To fabricate these materials with high quality, monodisperse silica nanoparticles were well dispersed in a pregel solution with volume fractions above 0.12. The pregel solution was composed of poly(ethylene

Received: October 8, 2013
Published: January 17, 2014

glycol) diacrylate (PEGDA, 10%, v/v), polyethylene glycol (PEG, 5%, v/v), and the photoinitiator 2-hydroxy-2-methyl-1-phenyl-1-propanone (HMPP, 1%, v/v). After the ion exchange process, interparticle repulsion occurs at the average interparticle spacing, and the minimum energy configuration makes the silica nanoparticles self-assemble into ordered and non-close-packed colloidal crystal array structures in the solution.[18,29,30] The highly ordered nanoparticles imparted the pregel solution with brilliant structure colors, and the color of the solution could be adjusted by using different concentrations or sizes of the silica nanoparticles. To generate the polymer colloidal crystal films, a mold was constructed by using two flat slides and a rectangular-shaped spacer between the slides. The nanoparticle suspension was introduced into the mold and photopolymerized with UV irradiation in situ (Figure 1a). Based on the achieved colloidal PhC films, diffraction

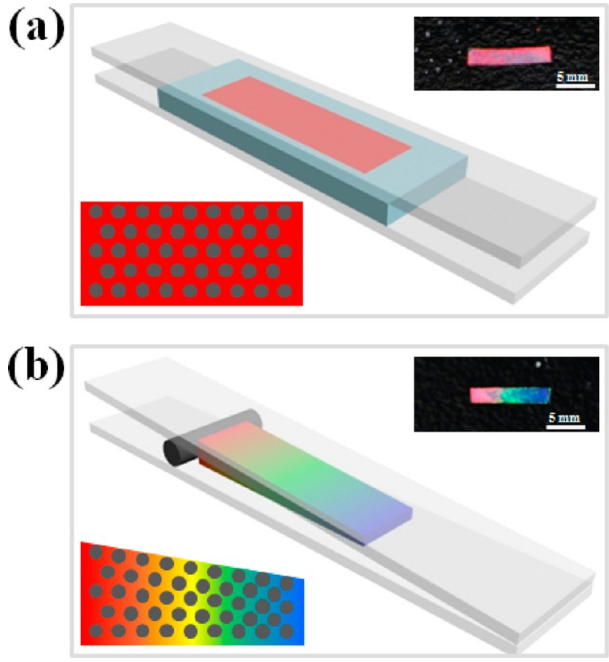

Figure 1. Schematic illustration of the fabrication of the spectrometer grating: (a) The SiO_2–PEGDA suspension was introduced into the cuboid mold and solidified by UV; (b) The obtained film was compressed by a tilted slide under a uniform force. The inset figures are the optical images of the films. The scale bars of the inset figures are 5 mm.

gratings with continuously varying PBGs could be generated by simply applying a pressure gradient to the films (Figure 1b). In our experiment, PEGDA was used to prepare the pregel solution. It could act not only as a monomer of the hydrogel, but also as the cross-linker. The addition of PEG could act as a dilution of PEGDA and reduce the degree of the cross-linking of PEGDA and make the hydrogel more elastic.

The microstructures of the polymer colloidal crystal films were characterized by scanning electron microscopy (SEM; Figure 2). It can be observed that the monodisperse silica nanoparticles on the film surface form a predominantly hexagonal symmetry (Figure 2a). This structure also extended internally to the whole film (Figure 2b). Because of the periodic arrangement of the silica nanoparticles, the resulting colloidal crystal films possess the PBG property. This property leads to certain wavelengths located in the PBG to be prohibited from

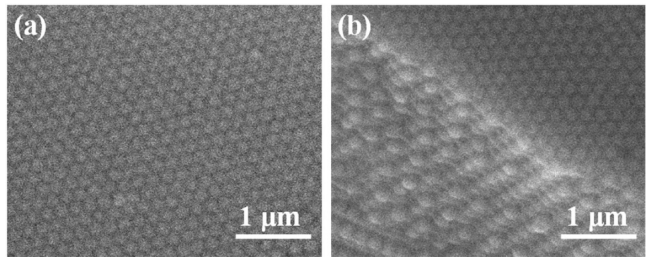

Figure 2. SEM images of the ordered silica colloidal crystal array in the hydrogel film: (a) Surface image; (b) Cross-sectional image.

propagating and thus be reflected from the films. Thus, the colloidal crystal films were imparted with vivid iridescent colors and characteristic reflection peaks.

The main peak position λ of the film could be estimated by Bragg's equation for a normal incident beam:[18,19,25]

$$\lambda = 2d_{111}n_{\text{average}} \quad (1)$$

where d_{111} is the interplanar distance of the (111) diffracting planes and n_{average} is the average refractive index of the colloidal crystal film, which was constant for the fixed film. Based on the equation, there are several protocols for tuning the PBGs of the films, such as changing the average refractive index or center distance of neighboring nanoparticles. Here, the polymer colloidal crystal films were composed of the PEG hydrogel network that was compressible, thus we employed a mechanical pressure to vary the (111) interplanar spacing and tune the PBGs of the films. In a certain range, different levels of pressure could cause different shift percentage (the extent of the PBG wavelength shift) of the PBGs of the film. Thus, to achieve the desired diffraction grating film with continuously varying PBGs, a pressure gradient was adopted in the elastic polymer colloidal crystal films. It is worth noting that if the film were tilted, the (111) planes would have been correspondingly tilted, and the detected value of the PBGs over the film surface would be influenced. Thus, the film and its (111) plane were kept perpendicular to the incident beam during the operations that followed, and the incident beam size was kept constant on the different positions of the film.

The relationships between different positions of the diffraction grating film and their corresponding PBGs were investigated. According to the geometric calculation, in the marked position (the detecting point is shown in Figure 3a) of the film, the thickness (h') under the compressed state is

$$h' = h - x^*\tan\alpha \quad (2)$$

where h is the initial thickness of the grating film, x is a variable length from the initiating terminal of the gradient pressure to the detected position, and α is the inclined angle of the gradient. On the other side, the thickness (h) was equal to the $d_{111} \times M$ (where M is the total number of layers of the colloidal crystal (111) diffraction plane, it was kept constant during the compressing operation). When the film the subjected to compression, the hydrogel film was under unidimentional deformation, leading to a decrease in thickness and in the lattice distance of (111) planes. In the diffraction grating film, the PBGs were mainly relative, with the distance of the (111) diffracting plane spacing, which appeared as the thickness of the film in macroscopic view, as deduced in eq 3:

$$h'/h = (d_{111}' \times M)/(d_{111} \times M) = \lambda'/\lambda_0 \quad (3)$$

dx.doi.org/10.1021/ph4000696 | ACS Photonics 2014, 1, 121−126

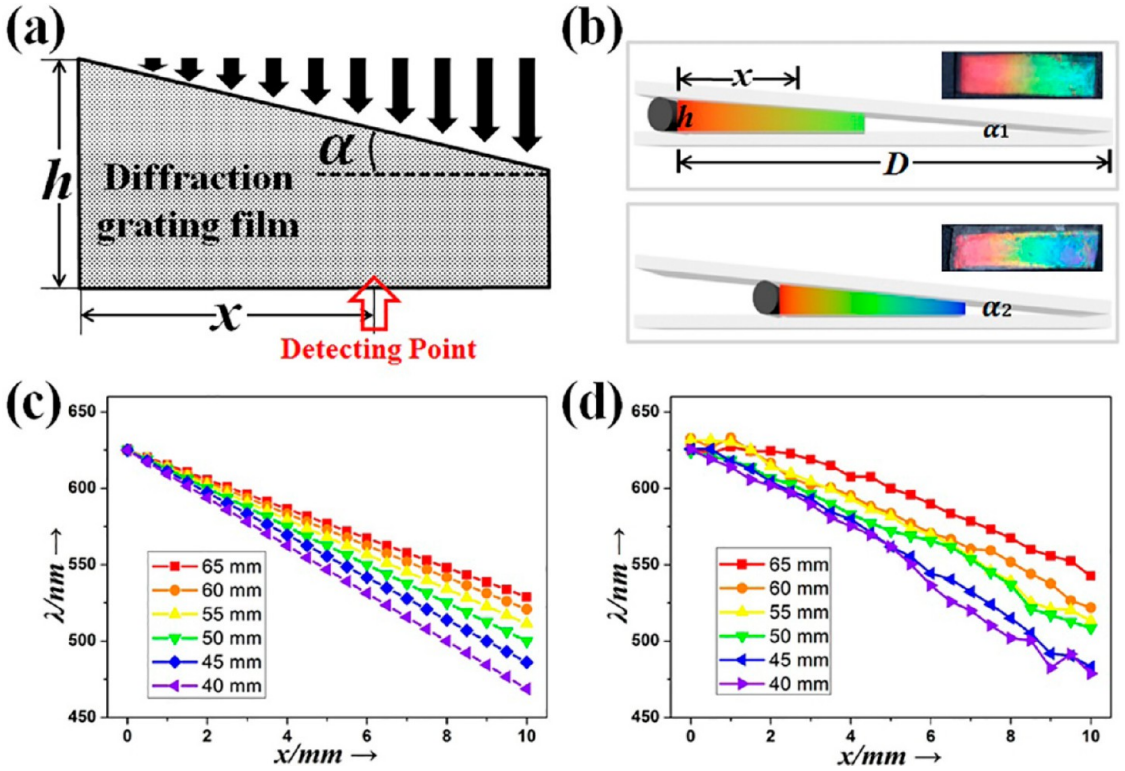

Figure 3. (a) Schematic for calculating the PBG wavelength at one position in the diffraction grating film. (b) Two examples of the grating films fabricated with different inclined angles, the larger inclined angle (below) resulted in a wider range of color gradient. (c, d) Relationships between the reflectance peaks and the position at six states: (c) calculated values and (d) detected values. The interval is 0.5 mm and the insets are the values of *D*. The boundaries of the film materials were immobilized during compression, and thus, the Poisson's ratio of this material has little effect on the grating.

where d_{111}' is the interplanar distance of the (111) diffracting planes at the detecting point, λ_0 and λ' are the characteristic reflection peak wavelength of the colloidal photonic crystal film at the initial and detecting points. By taking eq 2 into eq 3, the PBG wavelength (λ') of the detecting point was deduced as

$$\lambda' = \lambda_0(h - x \times \tan\alpha)/h \tag{4}$$

Based on eq 4, the detecting range could be expanded to the whole visible range. The maximum wavelength is restricted by the initial PBG of the colloidal photonic crystal film while the minimum wavelength is restricted by the limited compression ratio of the hydrogel and the diameter of the silica nanoparticles. From eq 4, it could be found that the other two intrinsic features of the grating film were the length and the thickness, which had effects on the detecting range and the resolution, respectively. On the other hand, the inclined angle has a remarkable influence on the resolution and detecting range of the grating, which should be considered for its contradictory effect. For the grating films with the same length and thickness, a bigger inclined angle would result in a wider detecting range while a lower resolution, as shown in Figure 3b.

Following the fabrication scheme (Figure 1b), the rectangular colloidal crystal film (10 mm long, 2 mm wide, and 250 μm thick) was placed beside the specialized rod spacer (250 μm diameter). A binder clip was chosen to clamp the slides at the other end so that the colloidal crystal film could be compressed under the pressure gradient resulting from the inclined angle between the slides. In Figure 3b, the distance (D) between the spacer and the binder clip could be used to adjust the inclined angle ($\tan\alpha = h/D$). Thus, eq 4 could be simplified to calculate the distribution of the PBGs in our diffraction grating film:

$$\lambda' = \lambda_0(1 - x/D) \tag{5}$$

From the equation it could be found that, for a fixed film with a given initial PBG and length of film, D was the only factor to tune the detecting range and the resolution of the diffraction grating film. Here, a series of detections were recorded to study the effects of D. For a grating film (10 mm in length), the arrangements of D for measuring the spectra were set at 5 mm intervals between 65 and 40 mm. The maximum compressing ratio of each state were 11.3, 12.3, 13.5, 14.9, 16.7, and 18.9%, respectively. The calculated and detected relationships between the reflectance peaks and the positions at six states were collected at distance intervals of 0.5 mm along the compression gradient. It was found that, for a grating film with fixed length and thickness, the distributed range of its PBGs increased with the decrease in D. However, the PBG resolution of the grating film was reduced when D became too small. In our experiment, because of the limited compression ratio of the polymer materials and the defects in the self-assembled colloidal crystals, the experimental results were not identical with the equations. Although the distributed range of the PBGs was less than the simulated results, the tendency of the experimental results was compatible with the equations. To further improve the equation, the practical equation for the PBGs across our grating film was adjusted by adding the coefficient (k) to offset the defect:

$$\lambda' = \lambda_0(1 - kx/D) \tag{6}$$

dx.doi.org/10.1021/ph4000696 | ACS Photonics 2014, 1, 121−126

Based on the detected value, the numerical values of k could be calculated as 1.021 by analyzing the linear equations in Figure 3d. Finally, an empirical law describing the relationship between the PBG wavelength (λ') and the detecting point (x) was achieved:

$$\lambda' = \lambda_0 - (1.021\lambda_0/D) \times x \quad (7)$$

Diffraction grating films should cover the whole visible range while keeping a high PBG resolution. The structural colors and the reflection peaks at different positions of the desired diffraction grating film (7.5 mm long) are given in Figure 4.

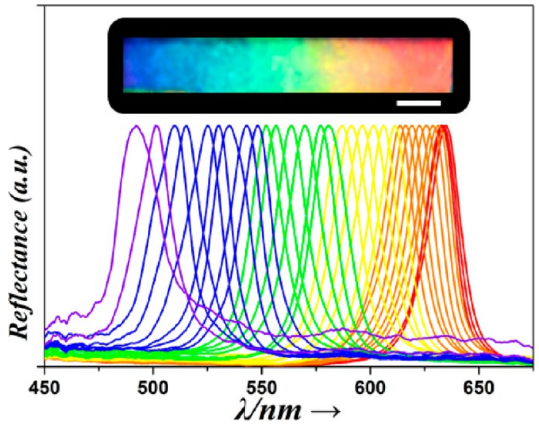

Figure 4. Optical image of a grating film with a black pane and the corresponding reflectance spectra (normalized) at intervals of 0.25 mm along the gradient direction. The scale bar is 1 mm.

The film showed a gradual change in the reflection color from red to blue, which indicates that the detecting range covers the whole visible range. The spectra were collected at local areas of round dots of 300 μm diameter at intervals of 0.25 mm along the film. The full width at half-maximum (fwhm) of the reflectance spectra was small, 16 nm in the red region and 23 nm in the blue region, indicating high PBG resolution of the new diffraction gratings. It could be seen that the detecting range of the spectrometer grating starts from an initial wavelength of 634 nm to a shorter wavelength of 491 nm. With a minimum scale value 10 μm of displacement, the PBG resolution could reach 0.19 nm (the minimal spectral shift value in a unit displacement for 7.5 mm grating film).

In the application of the diffraction grating films, their feature of spatially modulated reflectance spectra makes them novel diffraction gratings for spectrometers. Conventional spectrometer gratings split a light source into several beams with different propagation directions according to the wavelength, and the spectrometer need a detect array to acquire the intensity of different wavelength. Unlike the commercialized spectrometer gratings, our proposed system employed a continuously varying PBG film as the spectrometer grating, in which the reflection peaks varied with the positions. To demonstrate this application, a grating film was integrated into a miniaturized spectroscopic system with a photoelectric conversion module and a reflection probe (Figure 5a,b). The light was coupled from the source and then guided to the detecting head perpendicular to the grating film, where a part of the light was reflected and directed to the photoelectric conversion module. The photoelectric conversion module in this system could output a voltage to represent the reflected power, and a lower voltage corresponded to a stronger reflected

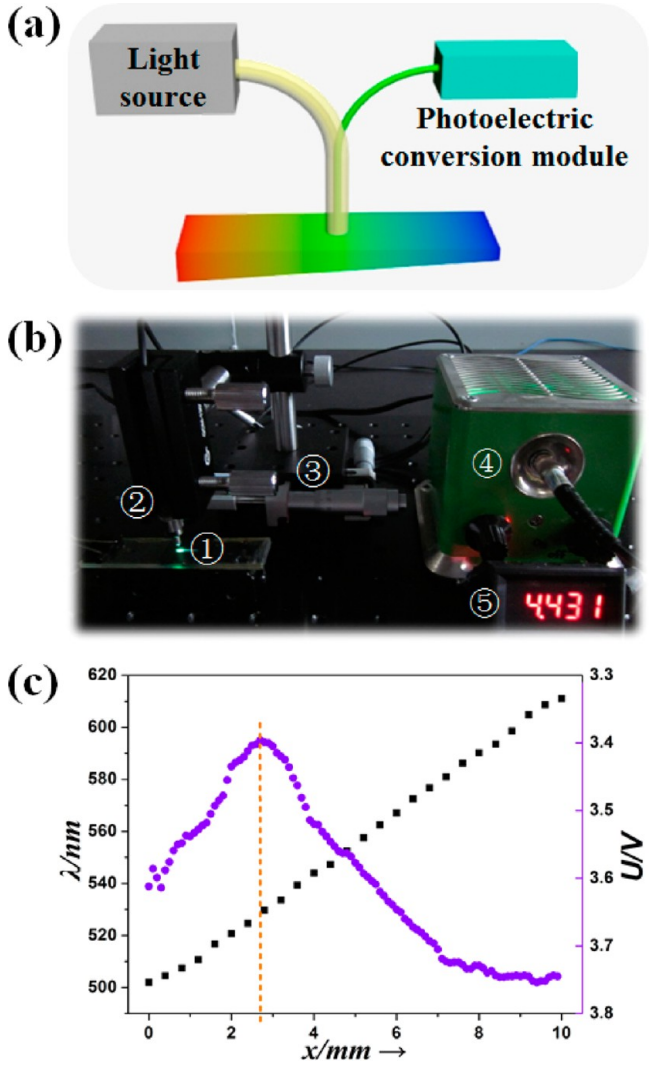

Figure 5. (a) Schematic illustration of the spectrometer system based on the colloidal crystal grating film. (b) Photograph of the spectrometer system: 1, grating film; 2, the detecting head (made of Y-type fiber); 3, translation stage; 4, light source; 5, photoelectric conversion module. (c) Plot (blue dots) of the reflectance power vs detection positions of the film at 0.1 mm intervals, and the relationships between the positions and the PBGs of the film (black squares) at 0.4 mm intervals. The reflectance power was expressed by a voltage that was detected by the photoelectric conversion module. When used in the spectroscopic system, the grating film could work a sealed water environment between the two slides (25 °C).

power. When the detecting head was moved along the compression gradient, the reflection intensities over the detecting range of the grating film were recorded and used to construct the spectrum of the input light. Here, an LED light source with the center wavelength at 530 nm was adopted as the detection object. The dots in Figure 5c show the relationships between the positions and the reflected intensity. It was found that the reflected power reached its maximum at the position of 2.7 mm. By referencing the above results about the relationships between the positions and the PBGs of the film (quadrates), it was found that the position of 2.7 mm corresponded to the PBG of 528.45 nm, indicating the high accuracy of our films in the miniaturized spectroscopic system.

In conclusion, we have demonstrated a practical strategy for the construction of novel spectrometer diffraction gratings

dx.doi.org/10.1021/ph4000696 | ACS Photonics 2014, 1, 121−126

based on stress-responsive colloidal photonic crystal films. The PBGs of the gratings could be tuned precisely by varying the level of pressure along the grating film. This imparts the grating films with the property of continuously varying PBGs over the visible range for light reflectance. By combining the achieved diffraction grating film with a photoelectric conversion module, we have demonstrated a miniaturized spectrometer system with the spectrum based on the reflection intensity profile at different spatial positions on the film. As our spectrometer gratings could satisfy the miniaturization demand for a spectroscopic system, it is expected that they would be integrated into other optical instruments and biosensors.

METHODS

Materials. Monodisperse silica nanoparticles with diameters of 180 nm were synthesized by the Stober-Fink-Bohn method.[31] The zeta potential of the charged silica nanoparticles was measured to be −55.2 mV in water. The colloidal silica nanoparticles were purified via centrifugation. The purified colloidal nanoparticles were dispersed in deionized water and shaken with an excess of ion-exchange resin (Bio-Rad AG501-X8(D)) to form iridescent colors with the assistance of sonication. Poly(ethylene glycol) diacrylates (PEGDA, M_w 700) and polyethylene glycol (PEG, M_w 200) was purchased from Alfa Aesar China Ltd., and the photoinitiator 2-hydroxy-2-methylpropiophenone (HMPP) was obtained from Sigma (St Louis, MO). The pregel solution was composed of poly(ethylene glycol) diacrylate (PEGDA, 10%, v/v), polyethylene glycol (PEG, 5%, v/v), the photoinitiator (HMPP, 1%, v/v), and the above colloidal crystal array solution. In a typical experiment, the concentration of silica nanoparticles in the pregel solution was 0.22 (v/v). After extensive mixing, 10% ion-exchange resin was added to the pregel solution. They were shaken together until strong structural color was visually evident. In our experiment, the desired final structural color was red. Then, the resin was removed by centrifuge.

Gratings Fabrication. A mold was prepared with two flat glass slides separated by a rectangle shape spacer (1 cm in length, 2 mm in width, and 250 μm in thickness). The pregel solution was introduced into the mold and then exposed to 365 nm UV light (EXFO OmniCure 1000) for 10 s. After the structure of the colloidal crystal stabilized, the rectangle shape spacer was removed. Then, one rod spacer (250 μm in diameter) was fixed between the slides, and the colloidal crystal film was placed beside the spacer. At last, a binder clip was used to clamp the slides on the other end. The PBG range and slop of the grating film could be tuned by adjusting the distance between the spacer and the binder clip. The grating film and the slides acted as a grating as a whole. When used in the spectroscopic system, the grating film could work in the sealed water environment between the two slides (25 °C). For a long time preservation, the grating film needed to be kept in water.

Characterization. The microstructure of the colloidal crystal film was characterized by SEM (HITACHI, S-300N) and the photographs of the colloidal crystal film were taken by an optical microscope (OLYMPUS, BX51) equipped with a CCD camera (Media Cybernetics Evolution MP 5.0). The reflection spectra of the colloidal crystal film were measured using a tungsten halogen source (Ocean Optics, LS-1) and an optical spectrometer (Ocean Optics, USB 2000).

Demonstration of the Spectroscopic System. The grating film was combined with a homemade photoelectric conversion module and a reflection probe (Y type). The photo photoelectric conversion module consisted of a miniature cadmium sulphide photoconductive cell (central wavelength: 540 nm) and a voltmeter module (voltage sensitivity: 0.001 V). The reflection probe had seven optical fibers (10 μm diameter) and six illumination fibers around one read fiber in a stainless ferrule. The ferrule was fixed on a translation stage and the minimum displacement scale value was 10 μm. The analyte light of narrow bandwidth (35 nm) was generated by a LED light source (Ocean Optics, LLS-530).

ASSOCIATED CONTENT

Supporting Information

Additional supporting figures. This material is available free of charge via the Internet at http://pubs.acs.org.

AUTHOR INFORMATION

Corresponding Author

*E-mail: yjzhao@seu.edu.cn; gu@seu.edu.cn.

Notes

The authors declare no competing financial interest.

ACKNOWLEDGMENTS

This research was supported by the National Natural Science Foundation of China (Grants 51073034, 21105011, and 50925309), the Natural Science Foundation of Jiangsu (Grant BK2012735), and the Program for Changjiang Scholars and Innovative Research Team in University (IRT1222). Y.J.Z. thanks the Program for New Century Excellent Talents in University.

REFERENCES

(1) Kumar, A.; Whitesides, G. M. Patterned condensation figures as optical diffraction gratings. *Science* **1994**, *263*, 60−62.
(2) Xia, Y.; Kim, E.; Zhao, X.; Rogers, J. A.; Prentiss, M.; Whitesides, G. M. Complex optical surfaces formed by replica molding against elastomeric matters. *Science* **1996**, *273*, 347−349.
(3) Ebbesen, T. W.; Lezec, H. J.; Ghaemi, H. F.; Thio, T.; Wolff, P. A. Extraordinary optical transmission through sub-wavelength hole arrays. *Nature* **1998**, *391*, 667−669.
(4) Harrison, G. R.; Loewen, E. G. Ruled gratings and wavelength tables. *Appl. Opt.* **1976**, *15*, 1744−1747.
(5) Lu, C.; Lipson, R. H. Interference lithography: a powerful tool for fabricating periodic structures. *Laser Photon. Rev.* **2010**, *4*, 568−580.
(6) Shukla, S.; Furlani, E. P.; Vidal, X.; Swihart, M. T.; Prasad, P. N. Two-photon lithography of sub-wavelength metallic structures in a polymer matrix. *Adv. Mater.* **2010**, *22*, 3695−3699.
(7) Viswanathan, N. K.; Kim, D. Y.; Bian, S.; Williams, J.; Liu, W.; Li, L.; Samuelson, L.; Kumar, J.; Tripathy, S. K. Surface relief structures on azo polymer films. *J. Mater. Chem.* **1999**, *9*, 1941−1955.
(8) Kang, D. J.; Bae, B. Photo-imageable sol−gel hybrid materials for simple fabrication of micro-optical elements. *Acc. Chem. Res.* **2007**, *40*, 903−912.
(9) Velev, O. D.; Kaler, E. W. Structured porous materials via colloidal crystal templating: from inorganic oxides to metals. *Adv. Mater.* **2000**, *12*, 531−534.
(10) Wong, S.; Kitaev, V.; Ozin, G. A. Colloidal crystal films: advances in universality and perfection. *J. Am. Chem. Soc.* **2003**, *125*, 15589−15598.
(11) Zhang, G.; Wang, D.; Möhwald, H. Patterning microsphere surfaces by templating colloidal crystals. *Nano Lett.* **2005**, *5*, 143−146.
(12) Yin, Y.; Alivisatos, A. P. Colloidal nanocrystal synthesis and the organic−inorganic interface. *Nature* **2005**, *437*, 664−670.
(13) Zhang, G.; Wang, D.; Möhwald, H. Fabrication of multiplex quasi-three-dimensional grids of one-dimensional nanostructures via stepwise colloidal lithography. *Nano Lett.* **2007**, *7*, 3410−3413.

(14) Xia, Y.; Gates, B.; Yin, Y.; Lu, Y. Monodispersed colloidal spheres: old materials with new applications. *Adv. Mater.* **2000**, *12*, 693−713.
(15) Galisteo-López, J. F.; Ibisate, M.; Sapienza, R.; Froufe-Pérez, L. S.; Blanco, Á.; López, C. Self-assembled photonic structures. *Adv. Mater.* **2011**, *23*, 30−69.
(16) López, C. Materials aspects of photonic crystals. *Adv. Mater.* **2003**, *15*, 1679−1704.
(17) He, L.; Hu, Y.; Kim, H.; Ge, J.; Kwon, S.; Yin, Y. Magnetic assembly of nonmagnetic particles into photonic crystal structures. *Nano Lett.* **2010**, *10*, 4708−4714.
(18) Ge, J.; Yin, Y. Responsive photonic crystals. *Angew. Chem., Int. Ed.* **2011**, *50*, 1492−1522.
(19) Zhao, Y. J.; Xie, Z. Y.; Gu, H. C.; Zhu, C.; Gu, Z. Z. Bio-inspired variable structural color materials. *Chem. Soc. Rev.* **2012**, *41*, 3297.
(20) Blannco, A.; Chomski, E.; Grabtchak, S.; Ibisate, M.; John, S.; Leonard, S. W.; López, C.; Meseguer, F.; Mîguez, H.; Mondia, J. P.; Ozin, G. A.; Toader, O.; van Driel, H. M. Large-scale synthesis of a silicon photonic crystal with a complete three-dimensional bandgap near 1.5 μm. *Nature* **2000**, *405*, 437−440.
(21) Li, H.; Wang, J.; Lin, H.; Xu, L.; Xu, W.; Wang, R.; Song, Y.; Zhu, D. Amplification of fluorescent contrast by photonic crystals in optical storage. *Adv. Mater.* **2010**, *22*, 1237−1241.
(22) Kim, S. H.; Hwang, H.; Yang, S. M. Fabrication of robust optical fibers by controlling film drainage of colloids in capillaries. *Angew. Chem., Int. Ed.* **2012**, *51*, 3661−3665.
(23) Lee, H. S.; Shim, T. S.; Hwang, H.; Yang, S. M.; Kim, S. H. Colloidal photonic crystals toward structural color palettes for security materials. *Chem. Mater.* **2013**, *25*, 2684−2690.
(24) Asher, S. A.; Sharma, A. C.; Goponenko, A. V.; Ward, M. M. Photonic crystal aqueous metal cation sensing materials. *Anal. Chem.* **2003**, *75*, 1676−1683.
(25) Lawrence, J. R.; Ying, Y.; Jiang, P.; Foulger, S. H. Dynamic tuning of organic lasers with colloidal crystals. *Adv. Mater.* **2006**, *18*, 300−303.
(26) Tian, E.; Wang, J.; Zheng, Y.; Song, Y.; Jiang, L.; Zhu, D. Colorful humidity sensitive photonic crystal hydrogel. *J. Mater. Chem.* **2008**, *18*, 1116−1122.
(27) Zhao, Y. J.; Zhao, X.; Tang, B.; Xu, W.; Li, J.; Hu, J.; Gu, Z. Z. Quantum-dot-tagged bioresponsive hydrogel suspension array for multiplex label-free DNA detection. *Adv. Funct. Mater.* **2010**, *20*, 976−982.
(28) Ye, B. F.; Zhao, Y. J.; Cheng, Y.; Li, T. T.; Xie, Z. Y.; Zhao, X. W.; Gu, Z. Z. Colorimetric photonic hydrogel aptasensor for the screening of heavy metal ions. *Nanoscale* **2012**, *4*, 5998−6003.
(29) Sato, O.; Kubo, S.; Gu, Z. Z. Structural color films with lotus effects, superhydrophilicity, and tunable stop-bands. *Acc. Chem. Res.* **2009**, *42*, 1−10.
(30) Zhao, Y. J.; Zhao, X.; Gu, Z. Z. Photonic crystals in bioassays. *Adv. Funct. Mater.* **2010**, *20*, 2970−2988.
(31) Stober, W.; Fink, A.; Bohn, E. Controlled growth of monodisperse silica spheres in the micron size range. *J. Colloid Interface Sci.* **1968**, *26*, 62−69.